Measurement of the $\eta \to 3\pi^0$ slope parameter α with the KLOE detector

F. Ambrosino[d,e,*], A. Antonelli[a], M. Antonelli[a], F. Archilli[i,j], P. Beltrame[c], G. Bencivenni[a], C. Bini[g,h], C. Bloise[a], S. Bocchetta[k,l], F. Bossi[a], P. Branchini[l], P. Campana[a], G. Capon[a], T. Capussela[d,*], F. Ceradini[k,l], P. Ciambrone[a], E. De Lucia[a], A. De Santis[g,h], P. De Simone[a], G. De Zorzi[g,h], A. Denig[c], A. Di Domenico[g,h], C. Di Donato[e], B. Di Micco[k,l], M. Dreucci[a], G. Felici[a], A. Ferrari[a], S. Fiore[g,h], P. Franzini[g,h], C. Gatti[a], P. Gauzzi[g,h], S. Giovannella[a], M. Jacewicz[a], W. Kluge[b], V. Kulikov[o], J. Lee-Franzini[a,m], M. Martini[a,f], P. Massarotti[d,e], S. Meola[d,e], S. Miscetti[a], M. Moulson[a], S. Müller[c], F. Murtas[a], M. Napolitano[d,e], F. Nguyen[k,l], M. Palutan[a], A. Passeri[l], V. Patera[a,f], F. Perfetto[d,e,*], P. Santangelo[a], B. Sciascia[a], A. Sciubba[a,f], T. Spadaro[a], C. Taccini[k,l], L. Tortora[l], P. Valente[h], G. Venanzoni[a], R.Versaci[a,f], G. Xu[a,n]

[a] *Laboratori Nazionali di Frascati dell'INFN, Frascati, Italy.*
[b] *Institut für Experimentelle Kernphysik, Universität Karlsruhe, Germany.*
[c] *Institut für Kernphysik, Johannes Gutenberg - Universität Mainz, Germany.*
[d] *Dipartimento di Scienze Fisiche dell'Università "Federico II", Napoli, Italy*
[e] *INFN Sezione di Napoli, Napoli, Italy*
[f] *Dipartimento di Energetica dell'Università "La Sapienza", Roma, Italy.*
[g] *Dipartimento di Fisica dell'Università "La Sapienza", Roma, Italy.*
[h] *INFN Sezione di Roma, Roma, Italy.*
[i] *Dipartimento di Fisica dell'Università "Tor Vergata", Roma, Italy.*
[j] *INFN Sezione di Roma Tor Vergata, Roma, Italy.*
[k] *Dipartimento di Fisica dell'Università "Roma Tre", Roma, Italy.*
[l] *INFN Sezione di Roma Tre, Roma, Italy.*
[m] *Physics Department, State University of New York at Stony Brook, USA.*
[n] *Institute of High Energy Physics of Academica Sinica, Beijing, China.*
[o] *Institute for Theoretical and Experimental Physics, Moscow, Russia.*

[*] Corresponding authors
Email addresses: Fabio.Ambrosino@na.infn.it (F. Ambrosino), Tiziana.Capussela@na.infn.it (T. Capussela), Francesco.Perfetto@na.infn.it (F. Perfetto)

Abstract

We present a measurement of the slope parameter α for the $\eta \to 3\pi^0$ decay, with the KLOE experiment at the DAΦNE ϕ-factory, based on a background free sample of ~ 17 millions η mesons produced in ϕ radiative decays. By fitting the event density in the Dalitz plot we determine $\alpha = -0.0301 \pm 0.0035\, stat\, ^{+0.0022}_{-0.0035}\, syst$. The result is in agreement with recent measurements from hadro- and photo-production experiments.

Keywords: e^+e^- collisions, ϕ radiative decays, η decays
PACS: 12.15Ff, 14.40Aq, 13.25JX

---

1. Introduction

The decay $\eta \to 3\pi$, $\pi^+\pi^-\pi^0$ and $3\pi^0$, though is a major decay mode of the η meson, violates isospin symmetry. Since contributions from the electromagnetic interaction are strongly suppressed by chiral symmetry [1] this decay is mainly due to the isospin breaking part of the QCD Lagrangian:

$$\mathcal{L}_I = -\frac{1}{2}\left(m_u - m_d\right)\left(\bar{u}u - d\bar{d}\right) \tag{1}$$

so that in principle it offers a way to determine the mass difference of the up-down quarks. Moreover, the selection rule $\Delta I = 1$ allows us to relate the amplitudes for the two decays using isospin symmetry:

$$A_{000}\left(s,t,u\right) = A_{+-0}\left(s,t,u\right) + A_{+-0}\left(t,u,s\right) + A_{+-0}\left(u,s,t\right) \tag{2}$$

Theoretical predictions for the decay amplitude have been obtained in the framework of Chiral Perturbation Theory (ChPT): the low energy effective field theory for QCD. Leading order (LO) ChPT predictions [2] based on current algebra underestimate the η decay rates by a factor of $\simeq 4$. One loop (NLO) calculations which include the $\pi - \pi$ rescattering effects [3] predict higher rates but still below the observed values. Some improvements are obtained by computing unitary corrections [4] to NLO using a dispersion relation for the decay amplitude derived by Khuri and Treiman [5]. Recently, more advanced calculations have become available. In reference [6] the authors use U(3) ChPT, in combination with a coupled channels method, and treat final state interactions by means of the Bethe Salpeter equation obtaining good agreement with measured decay widths and spectral shapes. In

Reference [7] a full NNLO computation is performed showing sizable corrections to the NLO result.
The Dalitz plot of a three body decay is described by two kinematical variables which for three identical particles in the final state, reduce to a single. In the $\eta \to 3\pi^0$ decay this variable is chosen by convention to be:

$$z = \frac{2}{3} \sum_{i=1}^{3} \left(\frac{3E_i - m_\eta}{m_\eta - 3m_{\pi^0}} \right)^2 , \tag{3}$$

where E_i denote the energy of the i-th pion in the η rest frame (CM). The variable z lies in the interval $[0-1]$, where $z = 0$ corresponds to events with 3 π^0 having all the same energy while for $z = 1$ one π^0 is at rest and the remaining two are emitted back to back.
The decay amplitude is represented at leading order in terms of a single quadratic slope parameter α:

$$|A_{000}(z)|^2 \sim 1 + 2\alpha z. \tag{4}$$

In case of pure phase space (i.e. at leading order in ChPT) one has $\alpha = 0$ and the z distribution is flat from $z = 0$ to $z \sim 0.76$ and then falls to zero at $z = 1$, see Fig. 1.

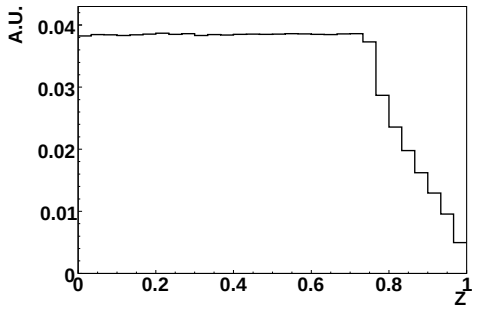

Figure 1: Expected z distribution for pure phase space.

Recent measurements of α with η-mesons produced almost at rest in hadro- and photo-production experiments are reported in Table 1. In the same Table are also shown the theoretical estimates for α previously described. The predicted values show differences - due to large cancellations in the amplitude computation - even quoting in some case a positive sign for α contrary

	α
Crystal Ball (2001) [8]	-0.031 ± 0.004
CELSIUS WASA [9]	-0.026 ± 0.014
WASA at COSY [10]	-0.027 ± 0.009
Crystal Ball at MAMI-B [11]	-0.032 ± 0.003
Crystal Ball at MAMI-C [12]	-0.032 ± 0.003
ChPT / LO	0.000
ChPT / NLO [3]	0.015
ChPT / NLO + unit. corrections [4]	-0.014 ÷ -0.007
U(3) ChPT + Bethe Salpeter [6]	-0.031 ± 0.003
ChPT / NNLO [7]	0.013 ± 0.032

Table 1: Experimental and theoretical results for the slope parameter α.

to the experimental evidence. A precise measurement of α therefore poses a significant constraint to theoretical models. We present a new measurement of α based on a large sample of η mesons produced in e^+e^- collisions via the radiative decay $\phi \to \eta\gamma$.

2. DAΦNE and KLOE

Data were collected with the KLOE detector at DAΦNE [13], the Frascati e^+e^- collider, which operates at a center of mass energy $W = m_\phi \sim 1020$ MeV. The beams collide with a crossing angle of $\pi - 25$ mrad, producing ϕ mesons with a small transverse momentum , $p_\phi \sim 13$ MeV/c. The KLOE [14] detector is inserted in a 0.52 T magnetic field and it consists of a large cylindrical drift chamber (DC), surrounded by a fine sampling lead-scintillating fibers electromagnetic calorimeter (EMC). The DC [15], 4 m diameter and 3.3 m long, has full stereo geometry and operates with a gas mixture of 90% helium and 10% isobutane. Momentum resolution is $\sigma(p_\perp)/p_\perp \leq 0.4\%$. Position resolution in $r - \phi$ is 150 μm and $\sigma_z \sim 2$ mm. Charged tracks vertices are reconstructed with an accuracy of ~ 3 mm.
The EMC [16] is divided into a barrel and two endcaps, and covers 98% of the solid angle. It is segmented into 2440 cells of cross section $\sim 4.4 \times 4.4$ cm^2 in the plane perpendicular to the fibers. Each cell is read out at both ends by photomultiplier tubes.

Arrival times of particles and space positions of the energy deposits are obtained from the signals collected at the two ends; cells close in time and space are grouped into a calorimeter cluster. The cluster energy E is the sum of the cell energies, while the cluster time t and its position r are energy weighted averages. The energy and time resolutions are respectively $\sigma_E/E = 5.7\%/\sqrt{E\ (\mathrm{GeV})}$ and $\sigma_t = 57\ \mathrm{ps}/\sqrt{E\ (\mathrm{GeV})} \oplus 100\ \mathrm{ps}$. Cluster positions are measured with a resolution of 1.3 cm in the coordinate transverse to the fibers, and, by timing, of 1.2 $\mathrm{cm}/\sqrt{E\ (\mathrm{GeV})}$ in the longitudinal coordinate.
The KLOE trigger [17] is based on the coincidence of two energy deposits with $E > 50$ MeV in the barrel and $E > 150$ MeV in the endcaps. Moreover, to reduce the trigger rate due to cosmic rays crossing the detector, events with a large energy release in the outermost calorimeter planes are vetoed.

3. Event selection

The measurement is based on an integrated luminosity of 420 pb^{-1} corresponding to $\simeq 1.4 \cdot 10^9$ ϕ mesons produced. This data sample contains about 17 millions of η mesons.
The detector response to the decay of interest was studied by using the KLOE MonteCarlo (MC) simulation program [18]. The MC takes into account variations in the machine operation and background conditions on a run-by-run basis. A MC sample for both signal and backgrounds was produced for an integrated luminosity five times that of the collected data. In the MC simulation of the $\eta \to 3\pi^0$ decay, the signal has been generated using our preliminary measurement [19] of $\alpha = -0.027$.
We search for: $\phi \to \eta\gamma$ with $\eta \to \pi^0\,\pi^0\,\pi^0$ and $\pi^0 \to \gamma\gamma$ events. To select the final state, we require to have seven prompt photons in the event. A photon is defined as an EMC cluster not associated to a DC track. We further require that $|(t - r/c)| < 5\sigma_t$, where t is the arrival time at the EMC, r is the distance of the cluster from interaction point, IP, c is speed of light. Fig. 2 shows the photon energy spectrum. The recoil photon from the two body decay $\phi \to \eta\gamma$ is almost monochromatic, with $E_{\gamma\,rec} \simeq 363$ MeV and separated from the softer photons from π^0 decay.
All events must pass a first-level selection to filter machine background and an event classification procedure [18]. Events with the expected final state signature are selected by requiring:

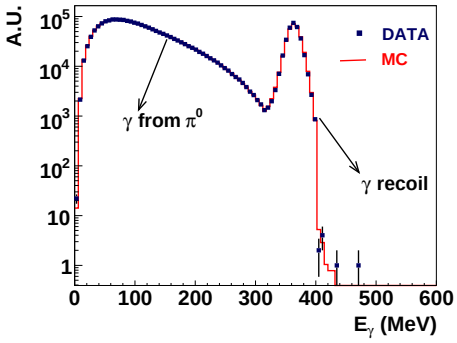

Figure 2: Photon energy spectrum in the laboratory. (Dots: data, histogram: MC).

- 7 and only 7 prompt photons with $21^\circ < \theta_\gamma < 159^\circ$ and $E_\gamma > 10$ MeV. The angle between any photon pair, $\theta_{\gamma\gamma}$, must be $> 9^\circ$ to reduce split showers. After these selection cuts we are left with $\simeq 4.6 \cdot 10^6$ events.

- A constrained kinematic fit imposing total 4−momentum conservation and $t = r/c$ for each photon is performed. Input variables to the fit are the energies, times of flight and the coordinates of clusters in the EMC and the beam energies. The fit improves the photon energies resolution: the π^0 mass resolution of ~ 15.4 MeV improves to ~ 9.6 MeV after applying the kinematic fit. The selected events must satisfy the requirement $P_{\chi^2} > 0.01$ corresponding to $\chi^2 < 25$. After this cut we are left with 1.9 millions of $\eta \to 3\pi^0$ events corresponding to a signal efficiency of $(40.81 \pm 0.01)\%$. At this level, the residual background contamination, mainly due to $K_S K_L$ decays to neutral channels, is estimated by MC to be $\sim 0.1\%$.

- To find the best combination (among 15) of the six less energetic photons into three π^0 a pairing procedure is applied. The procedure uses a pseudo-χ^2 variable:

$$\chi^2_j = \sum_{i=1}^{3} \left(\frac{m_{\gamma\gamma,ij} - m_{\pi^0}}{\sigma_{m_{\pi^0}}} \right)^2 \qquad j = 1, 2, \ldots, 15. \tag{5}$$

  where $m_{\gamma\gamma,ij}$ is the invariant mass of the i^{th} photon pair, in corrispondence of the j^{th} combination; $\sigma_{m_{\pi^0}}$ is the corresponding π^0 mass reso-

lution parametrized, as function of the photon energy resolution:

$$\frac{\sigma_{m_{\pi^0}}}{m_{\pi^0}} = \frac{1}{2}\left(\frac{\sigma_{E_{\gamma 1}}}{E_{\gamma 1}} \oplus \frac{\sigma_{E_{\gamma 2}}}{E_{\gamma 2}}\right), \tag{6}$$

the angular resolution contribution is negligible. In Fig. 3 a data-MC comparison of the minimum value of the pseudo-χ^2, χ^2_{min} is shown.

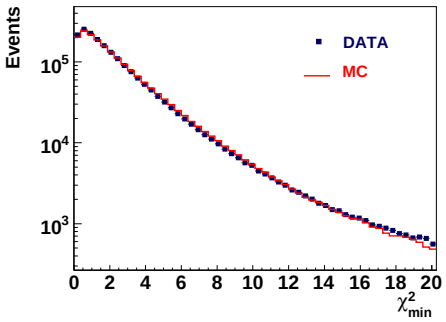

Figure 3: Distribution of χ^2_{min}, used to pair photons.(Dots: data, histogram: MC)

The fraction of events with correctly paired photons, estimated from MC, is named in the following as purity, P, of the data sample. While we define WPf = 1 - P the wrong pairing fraction to π^0's. To improve the purity a further cut is applied: $\chi^2_{min} < 5$. The distribution of the invariant mass of the two photons from π^0 decay, is shown in Fig. 4.

- After the photons pairing procedure a second kinematic fit is performed where the constraints on π^0 and η mass are also imposed. For the η mass we used the value $547.874 \pm 0.007\ stat\ \pm 0.031\ syst$ MeV measured by our experiment [20]. This fit improves the z resolution by a factor two.

We define three samples with different purity applying different cuts on the difference of the two lowest values of χ^2, $\Delta\chi^2$, as reported in Table 2. The resolution and efficiency as function of z are shown in Fig. 5 for the Medium purity sample. The reconstruction efficiency, $\varepsilon(z)$, is obtained by MC for each z bin, as the ratio: $\varepsilon(z) = N_{rec}(z)/N_{gen}(z)$ where $N_{gen,rec}$ are respectively the generated and reconstructed events.

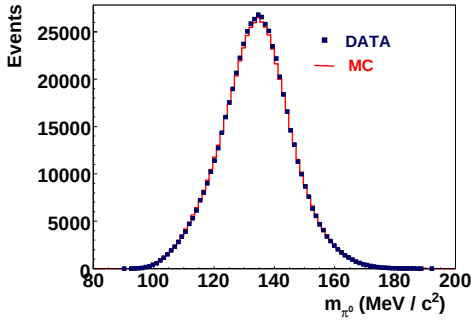

Figure 4: Invariant mass of the two photons from π^0 decay after cut $\chi^2_{min} < 5$. (Dots: data, histogram: MC).

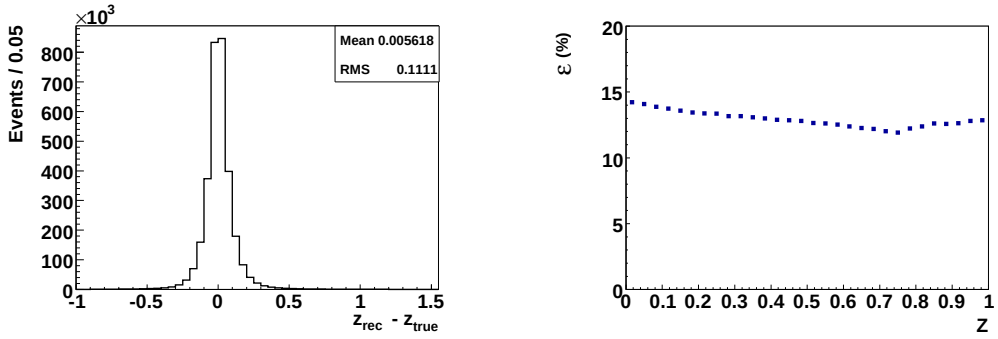

Figure 5: Medium purity sample. Left: Resolution on the z variable. Right: Reconstruction efficiency vs. z.

The photon energy resolution is compared between data and MC looking at the distribution of $\Delta E^*_\gamma = E^*_{\gamma_1} - E^*_{\gamma_2}$; i.e. the difference between photons energy in the π^0 rest frame. In Fig. 6 the distribution of ΔE^*_γ is plotted. Estimating the r.m.s. of the ΔE^*_γ for slices of 10 MeV in E_{π^0} a difference of ($1 \div 1.5$)% between data and MC is observed. Consequently, the MC photon energies have been smeared by this amount.
Fig. 7 shows the ratio $R_{\Delta E\gamma} = (\Delta E^*_\gamma)^{data}_{rms}/(\Delta E^*_\gamma)^{MC}_{rms}$. The correction improves the agreement between data and MC on this variable. The residual difference, of (0.6 ± 0.2)%, is taken into account directly in the evaluation of the result.

$\Delta\chi^2$ cut	Samples	Purity	Efficiency	N. events
2.5	Low	90.4 %	$(20.07 \pm 0.01)\%$	948471
5	Medium	95.0 %	(12.96 ± 0.01) %	614663
9	High	97.3 %	$(7.04 \pm 0.01)\%$	333493

Table 2: The three samples of different purity selected by different cuts on $\Delta\chi^2$.

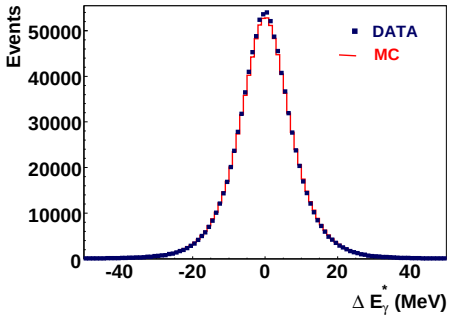

Figure 6: Plot of $\Delta E^*_\gamma = E^*_{\gamma_1} - E^*_{\gamma_2}$, where E^*_γ are the γ energies from π^0 decay in π^0 CM. (Dots: data, histogram: MC).

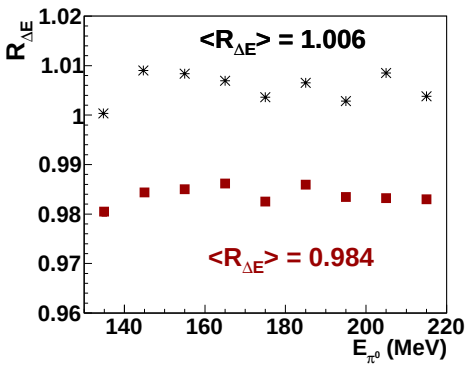

Figure 7: $R_{\Delta E}$: ratio of $(\Delta E^*_\gamma)^{data}_{rms}/(\Delta E^*_\gamma)^{MC}_{rms}$ vs. E_{π^0}. Dots (stars) before (after) the correction for the difference between Data and MC.

4. Measurement of the slope parameter α

The fit to the Dalitz plot is done minimizing a log–Likelihood function built as follows:

$$-\log \mathcal{L}(\alpha) = -\sum_{i=1}^{N_{bin}} n_i \log \nu_i(\alpha), \tag{7}$$

where, for each bin: n_i are the number of reconstructed events, ν_i the number of expected events, obtained from MC taking into account the detector resolution and WPf and weighted with $1+2\alpha z$. Moreover we correct for the data-MC differences in the WPf. To estimate it on data we use the distribution of z variable reconstructed using the second best pairing combination,$z_{\chi^2_2}$. This distribution is fit with the superposition of the MC shapes for events with good and wrong pairing respectively. The uncertainty on the WPf data-MC difference is taken into account in evaluating the systematic error.

The fit procedure has been tested on MC by verifying that the fit reproduces in output the same input value, within the statistical error.
To obtain the final result the fit range $(0 \div 0.7)$, corresponding to the region of the phase space in which the z distribution is flat, and the Medium purity sample is chosen. The fit results for the three different Purity samples are shown in Table 3. Moreover, we have applied a shift of $\Delta\alpha = -0.0008$ on the slope parameter α to correct the residual data-MC discrepancy in the photons energy resolution, see Section 3.

	Low Purity	**Medium Purity**	**High Purity**
$\alpha \cdot \mathbf{10^4}$	-319 ± 29	-301 ± 35	-308 ± 47
$\mathbf{P}_{\chi^2}$	92%	85%	91%

Table 3: α values from fit for different purity data samples.

In Fig. 8 a comparison between the observed and fitted z distributions is shown.

5. Systematic uncertainties

In the following we describe the sources of systematics. For each of them, the fit has been repeated varying the related sources and assuming as systematic error the difference with respect to the reference value. In Table 4 we have summarized all the systematic errors.

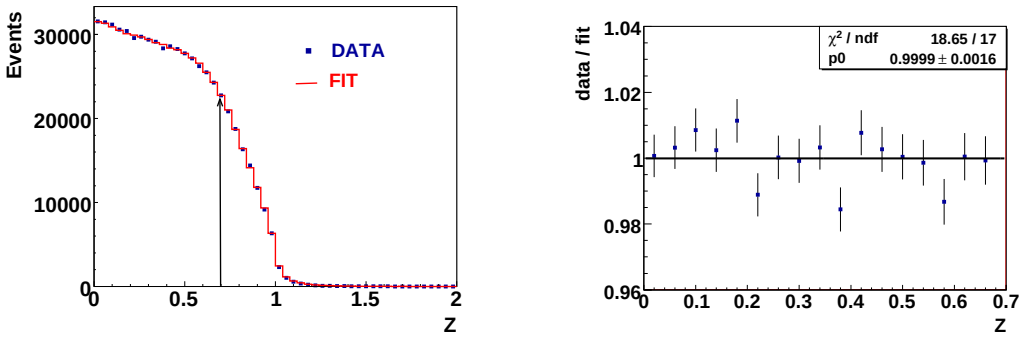

Figure 8: Medium purity sample: Left: observed z distribution with the corresponding fit overimposed. Right: data/fit ratio as function of z.

- **Analysis cuts** To control the stability of the result respect to our analysis cuts we have moved them independently. The cut on $\theta_{\gamma\gamma}$ to reject split showers,, was varied in the interval $6° - 18°$ in steps of $3°$. The photon energy threshold was also increased from 10 MeV to 40 MeV with a step of 5 MeV. The related systematic error is very small.

- **Energy Resolution** As shown in Fig. 7, the data-MC comparison of $(\Delta E^*_\gamma)_{rms}$ after correction shows a residual discrepancy of $(0.6 \pm 0.2)\%$. While the 0.6% correction has already been applied, we estimate the systematics related to its uncertainty to be $\Delta\alpha = \pm 3 \cdot 10^{-4}$.

- η **mass** This systematic effect has been estimated varying the η mass on data by ± 0.031 MeV accordingly to our measurement [20].

- **Wrong pairing fraction** For the sample used the data-MC ratio of WPf is 1.1 ± 0.1. As mentioned in Section 4 the fit procedure takes into account this difference. To assign the systematic error we repeated the fit procedure varying the WPf within the $\pm 10\%$ uncertainty quoted above.

- **Purity** As a check of the MC capability to reproduce the samples purity and its dependence upon z, we show in Fig. 9 the ratio between the number of events for the High and the Low purity sample, N_{High}/N_{Low}, as a function of z. A good agreement between data and MC throughout

the fit range is observed. As systematic error, we take the difference between the α values estimated using the Low and the High purity sample, see Table 3.

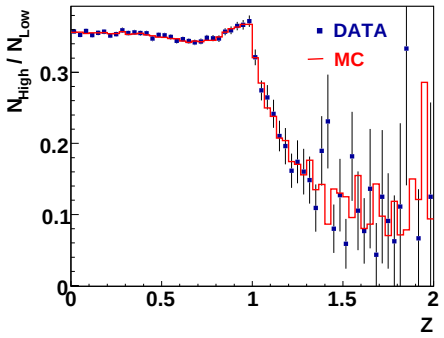

Figure 9: Ratio N_{high}/N_{low} as a function of z. (Dots: data, histogram: MC).

- **Fit range and binning** The fit was repeated with different values of the fit range from $[0 \div 0.6]$ to $[0 \div 1]$ with a step of 0.1. This is the largest systematic effect. Instead we find negligible effect when changing the bin size by a factor 2 from 0.04 to 0.02.

Source	$\Delta\alpha \cdot 10^4$	
Analysis cuts	-1	+1
Energy resolution	-3	+3
η Mass	-2	+6
Wrong pairing	-6	+5
Purity	-18	+0
Fit range	-29	+20
Total	-35	+22

Table 4: Summary of the systematic errors on the slope parameter α. The total systematic error is the sum in quadrature of the different contributions.

6. Conclusions

Using a clean sample of $\eta \to 3\pi^0$ decays we have measured the Dalitz Plot slope parameter obtaining $\alpha = -0.0301 \pm 0.0035\, stat\ ^{+0.0022}_{-0.0035}\, syst$ in agreement with other recent results of comparable precision.
The above value is also consistent with $\alpha = -0.038 \pm 0.003\, stat\ ^{+0.012}_{-0.008}\, syst$ obtained from the KLOE study of the $\eta \to \pi^+\pi^-\pi^0$ decay [21] using the theoretical correlations between the two decay modes.
Our α measurement confirms the inadequacy of simple NLO ChPT computations and the need to take into account higher order corrections.

Acknowledgements

We thank the DAFNE team for their efforts in maintaining low background running conditions and their collaboration during all data-taking. We want to thank our technical staff: G.F.Fortugno and F.Sborzacchi for their dedicated work to ensure an efficient operation of the KLOE computing facilities; M.Anelli for his continuous support to the gas system and the safety of the detector; A.Balla, M.Gatta, G.Corradi and G.Papalino for the maintenance of the electronics; M.Santoni, G.Paoluzzi and R.Rosellini for the general support to the detector; C.Piscitelli for his help during major maintenance periods. This work was supported in part by EURODAPHNE, contract FMRX-CT98-0169; by the German Federal Ministry of Education and Research (BMBF) contract 06-KA-957; by the German Research Foundation (DFG),'Emmy Noether Programme', contracts DE839/1-4; and by the EU Integrated Infrastructure Initiative HadronPhysics Project under contract number RII3-CT-2004-506078.

References

[1] D.G. Sutherland, Phys.Lett. 23 (1966) 384.

[2] J. Bijnens and J. Gasser, Physica Scripta T99 (2002) 34.

[3] J. Gasser and H. Leutwyler, Nucl. Phys. B 250 (1985) 539.

[4] J. Kambor, C. Wiesendanger, D. Wyler, Nucl. Phys. B 465 (1996) 215.

[5] N.N. Khuri and S.B. Treiman, Phys. Rev. 119 (1960) 1115.

[6] B. Borasoy and R. Nissler, Eur. Phys. J. A 26 (2005) 383.

[7] J. Bijnens and K. Ghorbani, JHEP 0711 (2007) 030.

[8] W.B. Tippens, et al.,Crystal Ball Collaboration, Phys. Rev. Lett. 87 (2001) 192001.

[9] M. Bashkanov, et al., CELSIUS/WASA Collaboration, Phys. Rev. C 76 (2007) 048201

[10] C. Adolph, et al., WASA-at-COSY Collaboration, Phys. Lett. B 677 (2009) 24.

[11] M. Unverzagt, et al., Crystal Ball at MAMI, TAPS and A2 Collaborations, Eur. Phys. J. A 39 (2009) 169.

[12] S. Prakhov, et al., Crystal Ball at MAMI and A2 Collaborations, Phys. Rev. C 79 (2009) 035204.

[13] M. Zobov, DAFNE Collaboration, Phys. Part. Nucl. Letters 5 (2008) 560.

[14] F. Bossi,E. De Lucia,J. Lee-Franzini, S. Miscetti, M. Palutan and KLOE Collaboration, Rivista del Nuovo Cimento Vol.31, N.10 (2008).

[15] M. Adinolfi, et al., Nucl. Instrum. Methods. A 488 (2002) 51.

[16] M. Adinolfi, et al., Nucl. Instrum. Methods. A 482 (2002) 364.

[17] M. Adinolfi, et al., Nucl. Instrum. Methods. A 492 (2002) 134.

[18] F. Ambrosino, et al., Nucl. Instrum. Methods. A 534 (2004) 403.

[19] F. Ambrosino, et al., KLOE Collaboration, arXiv: 0707.4137

[20] F. Ambrosino et al., KLOE Collaboration, JHEP 12 (2007) 073.

[21] F. Ambrosino et al., KLOE Collaboration, JHEP 05 (2008) 006.